Transmission coefficient from generalized Cantor-like potentials and its multifractality

Taichi Ogawana and Hidetsugu Sakaguchi
Department of Applied Science for Electronics and Materials, Interdisciplinary Graduate School of Engineering Sciences, Kyushu University, Kasuga, Fukuoka 816-8580, Japan

(Received 17 October 2017; published 12 January 2018)

We study the scattering problem at generalized Cantor-like potentials characterized by the expansion rate a and duplication number N, and derive an exact formula of transmittance. It was found that the transmittance is expressed with Chebyshev polynomials of the second kind, and the multifractality of the reflectance varies depending on a and N.

DOI: 10.1103/PhysRevE.97.012205

I. INTRODUCTION

The scattering and localization of electromagnetic waves and quantum mechanical waves in fractal media are an interesting topic [1,2]. Theoretically, several researchers studied electronic states and quantum localization in Sierpinski's gasket [3,4]. Experimentally, Takeda *et al.* reported the localization of electromagnetic waves when electromagnetic waves were irradiated to the Menger sponge [5]. As a simplest topic, many researchers studied the scattering process in the Cantor set by the transfer matrix method [6–16]. Using a recurrence relation, Sato *et al.* derived an exact formula for the reflectance of electromagnetic waves by the Cantor set [17]. The present authors derived a formula for the reflectance of quantum waves using the recurrence relation. Furthermore, they discussed a scaling law of the reflectance and the multifractality of the scaling function [18]. In this paper, we extend the results to generalized Cantor-like potentials. We show that the transmittance can be expressed using Chebyshev polynomials of the second kind, the scaling function is expressed by a finite product of the Laue function, and the multifractality depends on the shape of the generalized Cantor-like potentials.

II. TRANSMITTANCE FOR A PERIODIC ARRAY OF POTENTIAL BARRIERS

In this section, we briefly review the scattering problem by a periodic array of potential barriers [19]. The dimensionless Schrödinger equation is expressed as

$$-\frac{d^2\psi}{dx^2} + U(x)\psi = \varepsilon\psi, \tag{1}$$

where $U(x) = 2mV(x)/\hbar^2$, $\varepsilon = 2mE/\hbar^2$. First, we consider a case of a potential barrier of height U_0 in the interval $[0,L]$. The wave function of this system is represented by $\psi_l = A_l \exp(ikx) + B_l \exp(-ikx)\,(x < 0)$, $\psi_r = A_r \exp(ikx)$ $(x > L)$. The relationship between A_l, A_r, and B_l can be expressed as

$$\begin{pmatrix} A_l \\ B_l \end{pmatrix} = S(0,L)\begin{pmatrix} A_r \\ 0 \end{pmatrix} \tag{2}$$

using the transfer matrix S. S is written as

$$S(0,L) = \begin{pmatrix} s_{11}e^{ikL} & s_{21}^* e^{-ikL} \\ s_{21}e^{ikL} & s_{11}^* e^{-ikL} \end{pmatrix}, \tag{3}$$

$$s_{11} = \cos(qL) - i\cosh(v)\sin(qL), \tag{4}$$

$$s_{21} = -\sinh(v)\sin(qL), \tag{5}$$

where $k = \sqrt{\varepsilon}$, $q = \sqrt{\varepsilon - U(x)}$, $v = \ln(k/q)$, and v takes the principle value $-\pi/2 < \mathrm{Im}\, m(v) < \pi/2$. Reflectance and transmittance are defined as $R = |s_{21}/s_{11}|^2, T = |1/s_{11}|^2$ using the components of the transfer matrix. The transmittance is explicitly written as

$$T = \begin{cases} \left[1 + \left(\frac{k^2-q^2}{2kq}\right)^2 \sin^2 qL\right]^{-1} & (k < q), \\ \left[1 + \left(\frac{k^2+q^2}{2kq}\right)^2 \sinh^2 qL\right]^{-1} & (k > q). \end{cases} \tag{6}$$

Next, we consider a more general case where N potential barriers of height U_j locate at intervals $[x_j, x_j + d_j]$ $(j = 1,2,\dots,N)$, as shown in Fig. 1(a). The wave function of this system is denoted as $\psi_0 = A_0 \exp(ikx) + B_0 \exp(-ikx)$ $(x < x_0)$, $\psi_j = A_j \exp(ikx) + B_j \exp(-ikx)\,(x_j < x < x_j + d_j)$, $\psi_{N+1} = A_{N+1} \exp(ikx) + B_{N+1} \exp(-ikx)$ $(x > x_N + d_N)$. The relation

$$\begin{pmatrix} A_j \\ B_j \end{pmatrix} = S_{j+1}\begin{pmatrix} A_{j+1} \\ B_{j+1} \end{pmatrix} \tag{7}$$

is satisfied between the jth and $(j+1)$th wave functions. Considering that the transmitted wave of the jth potential becomes the incident wave of the $(j+1)$th potential, the relationship between (A_0,B_0) and (A_N,B_N) is expressed by the product of each transfer matrix S_j,

$$\begin{pmatrix} A_0 \\ B_0 \end{pmatrix} = S^{(N)}\begin{pmatrix} A_{N+1} \\ B_{N+1} \end{pmatrix} \equiv \prod_{j=1}^{N} S_j \begin{pmatrix} A_{N+1} \\ B_{N+1} \end{pmatrix}, \tag{8}$$

$$S^{(N)} = \begin{pmatrix} s_{11}^{(N)}e^{ikL} & s_{21}^{(N)*} e^{-ikL} \\ s_{21}^{(N)}e^{ikL} & s_{11}^{(N)*} e^{-ikL} \end{pmatrix}. \tag{9}$$

Reflectance and transmittance of this system can be defined by $R = |s_{21}^{(N)}/s_{11}^{(N)}|^2$, $T = |1/s_{11}^{(N)}|^2$. If the heights and widths

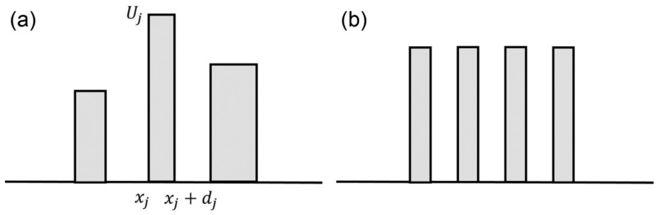

FIG. 1. (a) An array of N potential barriers. (b) A periodic array of potential barriers.

for potential barriers take the same values $U_j = U_0$ and $d_j = L$ for all j and the interval between neighboring potential barriers takes the same value $x_{j+1} - (x_j + d_j) = \Delta$ as shown in Fig. 1(b), the components of the transfer matrix S are expressed as

$$s_{11}^{(N)} = u_{N-1}(t)s_{11} - u_{N-2}(t)e^{ik\Delta},$$
$$s_{21}^{(N)} = u_{N-1}(t)s_{21}, \tag{10}$$

where u_j are Chebyshev polynomials of the second kind which satisfy the recurrence formula

$$u_j(t) = 2yu_{j-1}(t) - u_{j-2}(t) \quad (j = 0,1,\dots,N), \tag{11}$$

and

$$u_{j-1}(t) = \sin(jt)/\sin(t),$$
$$t = \cos^{-1}[|s_{11}|\cos(k\Delta - \theta)],$$
$$y = |s_{11}|\cos(k\Delta - \theta),$$
$$\theta = \arg(s_{11}).$$

Using these relations, the transmittance is written as

$$T = \left[1 + \sinh^2(v)\sin^2(qL)u_{N-1}^2(t)\right]^{-1} \quad (k > q). \tag{12}$$

If the wave number k of the wave function is large enough, the transmittance can be approximated at

$$T \simeq 1 - \left(\frac{U_0}{2k}\right)^2 \sin^2(kL)\left(\frac{\sin[Nk(L+\Delta)]}{\sin[k(L+\Delta)]}\right)^2, \tag{13}$$

because $\sinh(v) \sim U_0/2k$, $|s_{11}| \sim 1$, $|s_{21}| \sim 0$, $\theta \sim -kL$. Figure 2 shows the transmittance calculated by Eq. (14) for $N = 4$, 32, 264, and 1024. The other parameters are $L = 1$, $\Delta = 1$, $U_0 = 100$.

III. TRANSMITTANCE FOR N-DIVIDED CAnTOR-LIKE POTENTIAL USING RECURRENCE RELATION

The well-known 3-adic Cantor set is constructed by recursively repeating the operation of removing the central portion after dividing the line into three equal parts. The pre-Cantor sets of the nth stage are recursively expressed as follows,

$$C_n^{(3)} = \frac{C_{n-1}^{(3)}}{3} \cup \left(\frac{2}{3}L + \frac{C_{n-1}^{(3)}}{3}\right), \quad C_0^{(3)} = [0,L]. \tag{14}$$

We define a generalized Cantor set by the following operation. First, divide the basic line segment L equally $2N - 1$. Next, remove the line segments so that the line segments and the gaps alternate. Finally, the remaining line segment is multiplied by $1/a$ of the line segment before division and place them

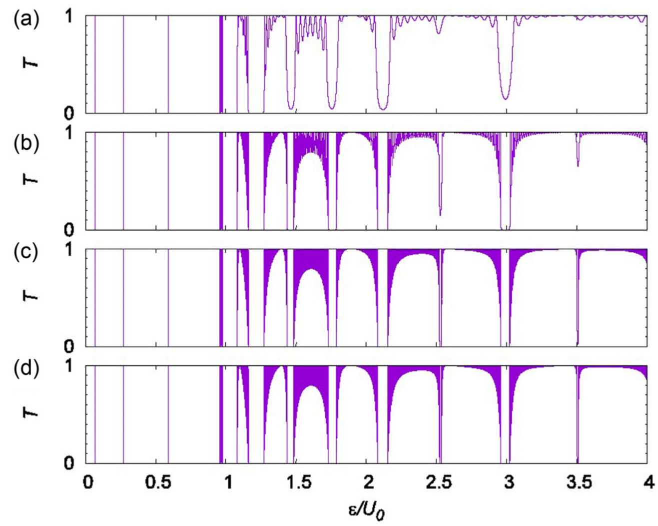

FIG. 2. Transmittance of a wave function incident on N number of equally spaced potentials. (a) $N = 4$. (b) $N = 32$. (c) $N = 264$. (d) $N = 1024$. The other parameters are $L = 1$, $\Delta = 1$, $U_0 = 100$.

at equal intervals $\Delta = (a - N)L/[a(N - 1)]$. We construct a pre-Cantor set of the nth stage by repeating the above operation. Schematic figures for the generalized Cantor set are shown in Fig. 3. The operation is expressed as follows,

$$C_n^{(N)} = \bigcup_{j=0}^{N-1}\left[\frac{a-1}{a(N-1)}jL + \frac{C_{n-1}^{(N)}}{a}\right], \quad C_0^{(N)} = [0,L], \tag{15}$$

where $2 \leqslant N < a$, $a \in \mathbb{Q}$, $N \in \mathbb{N}$. We study this generalized Cantor set of reduction rate $1/a$ and duplication number N. In this paper, we call this Cantor set the $(2N - 1)$-adic Smith-Volterra (SV) Cantor set, because a generalized Cantor set of $N = 2$ and $a \neq 3$ is called the Smith-Volterra Cantor set and another generalized Cantor set of $a = 2N - 1$ is called the $(2N - 1)$-adic Cantor set. The original 3-adic Cantor set corresponds to $a = 3$ and $N = 2$. The feature of this set is that the number of elements is N^n and the length is $(N/a)^n$ at generation n. The fractal dimension of this Cantor set is $\ln(N)/\ln(a)$.

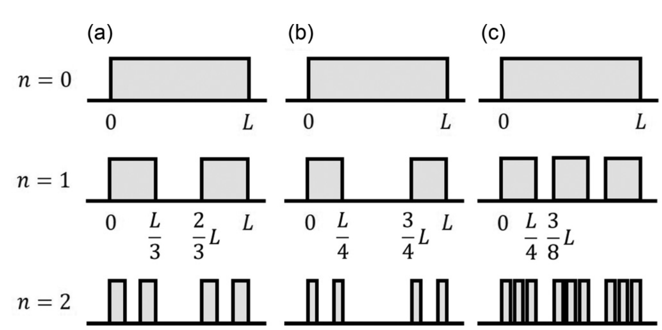

FIG. 3. Schematic diagram of the Cantor-like potentials in the n = zeroth, first, and second stage. (a) 3-adic Cantor-like potential barrier. (b) $(2N - 1)$-adic SV Cantor-like potential barrier for $a = 4$, $N = 2$. (c) $(2N - 1)$-adic SV Cantor-like potential barrier for $a = 4$, $N = 3$.

Here, we consider the scattering problem of a quantum mechanical particle incident into the generalized Cantor-like potential $U(x)$. A schematic figure of generalized Cantor-like potentials of several stages is shown in the Fig. 3.

The potential is located within an interval $[0,L]$ and takes a constant value U_0 on the $(2N-1)$-adic SV Cantor sets $x \in C_n^{(N)}$. The number of elements of the potential is N^n at the nth stage. The transmittance can be directly calculated by the product of N^n transfer matrices. However, it takes a very long time to calculate it in case of sufficiently large n. The calculation is simplified by deriving a recurrence relation for the transfer matrix using the self-similarity of the $(2N-1)$-adic SV Cantor set [17]. The recurrence relation on the transfer matrix is derived as follows. The wave function is expressed as $\psi_l = A_l \exp(ikx) + B_l \exp(-ikx)$ $(x < 0)$ and $\psi_r = A_r \exp(ikx) + B_r \exp(-ikx)$ $(x > L)$. The relationship between (A_r, B_r) and (A_l, B_l) is expressed as

$$\begin{pmatrix} A_l \\ B_l \end{pmatrix} = M_n(0,L) \begin{pmatrix} A_r \\ B_r \end{pmatrix} \tag{16}$$

using the transfer matrix of this system M_n. Because of the self-similarity of the $(2N-1)$-adic SV Cantor-like potential, the transfer matrix of the gth stage is expressed with the transfer matrix of the $(g-1)$th stage as

$$M_g(0,L) = \prod_{j=0}^{N-1} M_{g-1}(j\gamma/a,(j+1)\gamma/a) \tag{17}$$

where $\gamma = (a-1)L/(N-1)$. If the transfer matrix M_g is expressed as

$$M_g(0,L) = \begin{pmatrix} \xi_g e^{ikL} & \eta_g^* e^{-ikL} \\ \eta_g e^{ikL} & \xi_g^* e^{-ikL} \end{pmatrix}, \tag{18}$$

the parameters ξ_g and η_g satisfy the recurrence relation

$$\begin{aligned} \xi_g &= u_{N-1}(t_{g-1})\xi_{g-1} - u_{N-2}(t_{g-1})e^{ikw_{g-1}}, \\ \eta_g &= u_{N-1}(t_{g-1})\eta_{g-1} = \cdots = \eta_0 \prod_{j=0}^{g-1} u_{N-1}(t_j), \end{aligned} \tag{19}$$

where $g = 0,1,\ldots,n$, and

$$\begin{aligned} t_g &= \cos^{-1}[|\xi_g|\cos(kw_g - \theta_g)], \quad \theta_g = \arg(\xi_g), \\ w_g &= [(a-N)L]/[(N-1)a^{n-g}]. \end{aligned}$$

For $k > \sqrt{U_0}$, the initial values of ξ_g and η_g are given by

$$\begin{aligned} \xi_0 &= \cos(qL/a^n) - i\cosh(v)\sin(qL/a^n), \\ \eta_0 &= -i\sinh(v)\sin(qL/a^n), \end{aligned} \tag{20}$$

where $q = \sqrt{\varepsilon - U_0}$. Using these relations, the transmittance is written as

$$T = \left[1 + \sinh^2(v)\sin^2(qL/a^n)\prod_{j=0}^{n-1} u_{N-1}^2(t_j)\right]^{-1}. \tag{21}$$

The reflectance R is given by $R + T = 1$.

The behavior of this transmittance (21) can be approximated as follows at a sufficiently large wave number. If k is sufficiently large and $q/a^n \ll 1$, $|\eta_0| = \sinh(v)\sin(q/a^n) \ll 1$ and $|\xi_g| \sim 1$. Therefore, ξ_g can be approximated at $\xi_g \simeq e^{i\theta_g}$, where θ_g satisfies

$$\theta_{g+1} = N\theta_g + (N-1)w_g k. \tag{22}$$

The solution of this equation is $\theta_g = -(a^g - 1)/a^n$. Then, Chebyshev polynomials of the second kind are rewritten as

$$u_g(t_g) \simeq \frac{\sin(N\gamma k/a^{n-g})}{\sin(\gamma k/a^{n-g})}. \tag{23}$$

Additionally, using the relation of $q \sim k$, $\sinh(\nu) \sim U_0/2k$, $\sin(qL/a^n) \sim kL/a^n$, the transmittance is approximated as

$$T \sim 1 - \left(\frac{U_0 L}{2k}\right)^2 \left(\frac{N}{a}\right)^{2n} \prod_{j=1}^{n} \frac{\sin^2(N\gamma k/a^j)}{N^2 \sin^2(\gamma k/a^j)}. \tag{24}$$

As a result, the transmittance is composed of three elements: the first term of $(U_0 L/k)^2$, the second term of $(N/a)^{2n}$ derived from the length of the $(2N-1)$-adic SV Cantor set, and the third term derived from the resonance by the gaps between the elements of the $(2N-1)$-adic SV Cantor set. In the case of the 3-adic Cantor set of $a = 3$ and $N = 2$, $\gamma = 2L$ and $\sin^2(N\gamma k/a^j)/\{N^2\sin^2(\gamma k/a^j)\} = \sin^2(4kL/3^j)/\{4\sin^2(2kL/3^j)\} = \cos^2(2kL/3^j)$. Therefore, Eq. (24) leads to

$$T \sim 1 - \left(\frac{U_0 L}{2k}\right)^2 \left(\frac{N}{a}\right)^{2n} \prod_{j=1}^{n} \cos^2(2kL/3^j), \tag{25}$$

which recovers our previous result [18].

Now we can calculate the transmittance using Eq. (21); however, as increasing the stage number n, the transmittance approaches 1 for almost all k because the second term of Eq. (24) decreases as $(N/a)^{2n}$. To investigate the characteristic behavior of the transmittance for the $(2N-1)$-adic SV Cantor-like potential, we consider a potential which depends on the stage number n such as $U(x) = (a/N)^n U_0$ [18]. For this potential, the integral $\int_0^L U(x) = U_0 L$ is constant for any n. In these types of potentials, the transmittance $T(k)$ converges as $n \to \infty$. Then, the transmittance is approximate as

$$\begin{aligned} T &\sim 1 - \left(\frac{U_0 L}{2k}\right)^2 \prod_{j=1}^{n} \frac{\sin^2(N\gamma k/a^j)}{N^2 \sin^2(\gamma k/a^j)} \\ &= 1 - \left(\frac{U_0 L}{2k}\right)^2 G^{(n)}(k). \end{aligned} \tag{26}$$

The reflectance is given by $R = 1 - T \sim (U_0 L/2k)^2 G^{(n)}(k)$. Figure 4 shows the transmittance calculated by Eq. (21) for the tenth stage potential $U(x) = (a/N)^n U_0$. The parameters $L = 1$ and $U_0 = 512$, and the other parameters are $a = 3$, $N = 2$ [Fig. 4(a)], $a = 4$, $N = 2$ [Fig. 4(b)], $a = 4$, $N = 3$ [Fig. 4(c)], $a = 5$, $N = 2$ [Fig. 4(d)], $a = 5$, $N = 3$ [Fig. 4(e)], and $a = 5$, $N = 4$ [Fig. 4(f)]. The difference in these transmittances is due to the two parameters a and N.

The resonant scattering of this system appears in order from those of the structure of a low generation Cantor-like potential. The resonant scattering appears at a wave number that satisfies the following formula,

$$|\xi_g|\cos(kw_g - \theta_g) = \cos[(2m-1)\pi/N], \tag{27}$$

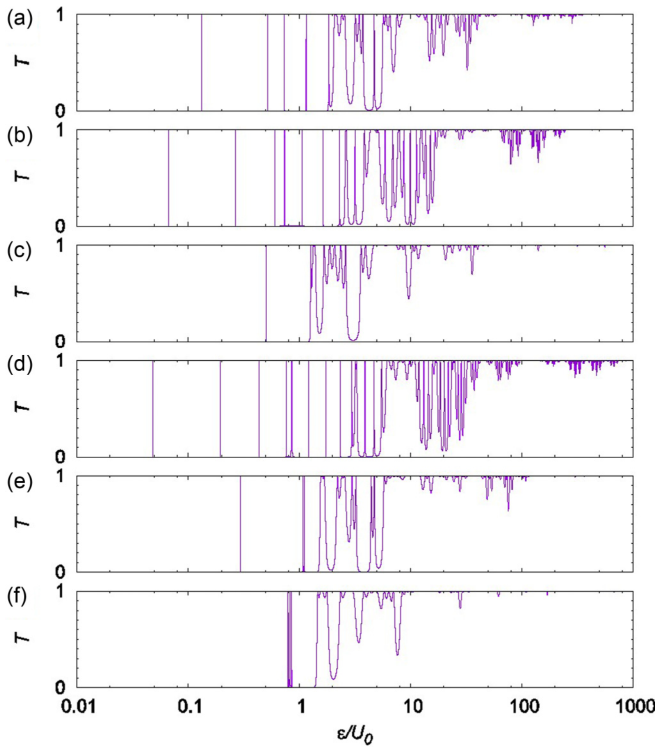

FIG. 4. Transmittance for the tenth stage potential $U(x) = (a/N)^n U_0$ at $L = 1$, $U_0 = 512$. (a) $a = 3$, $N = 2$. (b) $a = 4$, $N = 2$. (c) $a = 4$, $N = 3$. (d) $a = 5$, $N = 2$. (e) $a = 5$, $N = 3$. (f) $a = 5$, $N = 4$.

where $g = 0,1,\ldots,n$ and m is a integer other than a multiple of N. Sharp peaks for $\varepsilon/U_0 < 1$ correspond to the resonant tunneling, which can be observed even in the potential of the first generation. The number of peaks of the resonant scattering increases with a for a fixed value of $N = 2$, as is seen from Figs. 4(a), 4(b) and 4(d). The peak structure is not always simple, but has a finer structure. It is known that double or triple peaks appear in the transmission coefficient for the triple or quadruple potential walls which correspond to the potential of $N = 3$ or 4 in the first generation [20]. Even in our Cantor-like potentials of $N = 2$, 3, and 4, double peaks and triple peaks appear in the range of $\varepsilon/U_0 < 1$, as shown in Fig. 5. Figures 4(a)–4(f) are respectively the enlargement of Figs. 5(a)–5(f) for small ranges of $\varepsilon/U_0 < 1$.

Double peaks for $N = 2$ originate from the structure of generation 2. When ε/U_0 becomes sufficiently large, resonance scattering occurs at the zero point of the Laue function,

$$k = \frac{\pi a}{N\gamma} l, \tag{28}$$

from the approximation formula of Eq. (26), where l is an integer other than a multiple of N. At this time, the resonant scattering occurs periodically.

The Cantor-like potential can be constructed with various experimental protocols. In the experimental system, it is expected that it is difficult to create an ideal Cantor-like potential because of external fields and disorders. There are some studies that state that scaling laws in fractal lattices are sensitive to disorder and external fields [21]. To investigate an effect of the disorder, we have calculated the transmittances for $n = 10$, $a = 4$, $N = 3$ in two cases. In the first case, randomness is added to the potential height,

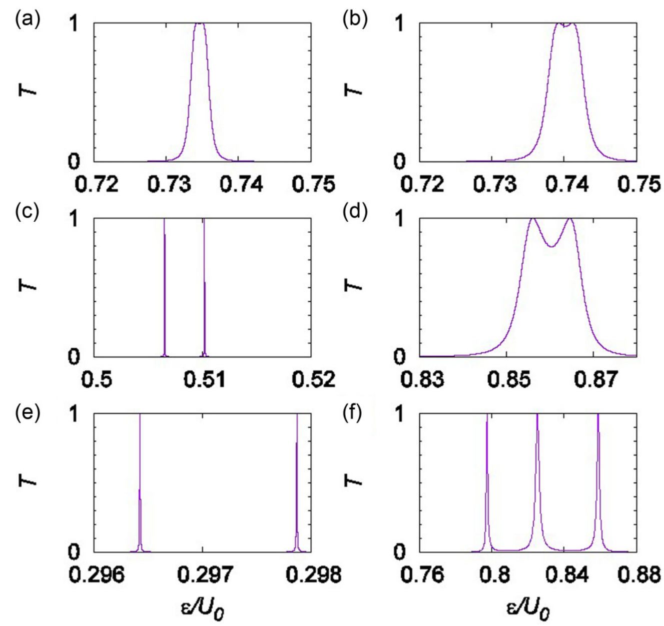

FIG. 5. Enlarged view of transmittance peak at $\varepsilon/U_0 < 1$. (a) $a = 3$, $N = 2$. (b) $a = 4$, $N = 2$. (c) $a = 4$, $N = 3$. (d) $a = 5$, $N = 2$. (e) $a = 5$, $N = 3$. (f) $a = 5$, $N = 4$.

$$\begin{pmatrix} A_0 \\ B_0 \end{pmatrix} = \prod_{j=1}^{N^n} S_j(xl_j, xr_j, k, q_j) \begin{pmatrix} A_{N+1} \\ B_{N+1} \end{pmatrix}, \tag{29}$$

where xl_j and xr_j are the left and right points of the jth potential, respectively, and $q_j = \sqrt{\varepsilon - (a/N)^n U_0(1 + p_1 W_j)}$, $0 < p_1 < 1$, where W_j is a random number between -0.5 and 0.5. In the second case, randomness is added to the position of the potential component,

$$\begin{pmatrix} A_0 \\ B_0 \end{pmatrix} = \prod_{j=1}^{N^n} S_j(xl_j + p_2, xr_j + p_2, k, q) \begin{pmatrix} A_{N+1} \\ B_{N+1} \end{pmatrix}, \tag{30}$$

where $p_2 = (a - N)/(N - 1) \times L/a^n \times W_j$. It is assumed that the width of the component of these potentials does not change. Figure 6 shows these potentials. The transmittance was calculated using the (1,1) component after calculating the finite product of the transfer matrix in formulas (29) and (30), respectively. Figure 7 shows the results of Eqs. (29) and (30). For $\varepsilon/U_0 < 1$, the transmittance is influenced by the external field as compared with the case where there is no fluctuation. On the other hand, when $\varepsilon/U_0 > 1$, disturbance of the peak due to fluctuation can be confirmed, but the behavior of the transmittance is almost the same as in the case without fluctuation.

The calculation of the transmittance using the recursive relation can be applied even when the potential height is not constant. Consider the $(2N-1)$-adic SV Cantor set with $N = 3$, as shown in Fig. 8(a). The integral of this potential $\int_0^L U(x) = U_0 L$ is constant. The difference from the previous

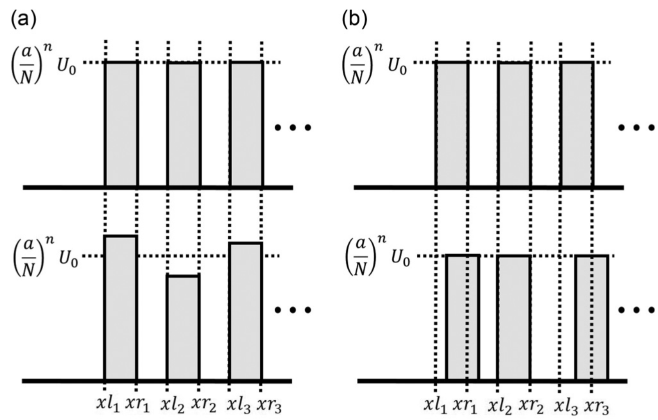

FIG. 6. (a) Cantor-like potential with randomness in the heights of elemental potential walls. (b) Cantor-like potential with randomness in the positions of elemental potential walls.

potential is that the potential height is multiplied by $(a-2)$ only for the middle line segment after dividing the line segment. In the case of such a potential, it is difficult to formulate an explicit mathematical expression such as Eq. (21) but a numerical calculation is easy. Figure 8(b) is a result of Eq. (21) at $a=4$, $N=3$, and Fig. 8(c) is a numerical calculation of the potential of Fig. 8(a). Figures 8(b) and 8(c) have the same potential integral value, but the behavior of the transmittance is different.

IV. MULTIFRACTALITY OF THE TRANSMITTANCE

Complex behaviors appear in the transmittance owing to the function $G(k)$, as shown in Fig. 4. Some features of $G(k)$ are discussed in the following. First of all, $G(k)$ satisfies $0 \leqslant G(k) \leqslant 1$. This is because $G(k)$ is a finite product of the Laue function defined by $L(x) = \sin^2(Nx)/\sin^2(x)$ (N is an integer). The Laue function is used in x-ray diffraction. The Laue function takes the minimum value 0 at $x = m\pi/N$ (where m is an integer other than a multiple of N), the maximum value

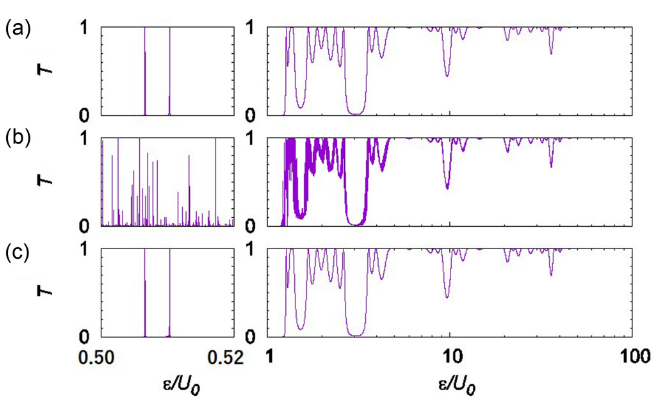

FIG. 7. Transmittance for the tenth stage potential $U(x) = (a/N)^n U_0$ at $a=4$, $N=3$, $L=1$, $U_0=512$. The left-hand side shows the transmittance near the wave number showing the resonant tunnel. The right-hand side shows the transmittance for $\varepsilon/U_0 > 1$. (a) Results for Eq. (21). (b) Results for Eq. (29) at $p_1 = 0.1$. (c) Results for Eq. (30).

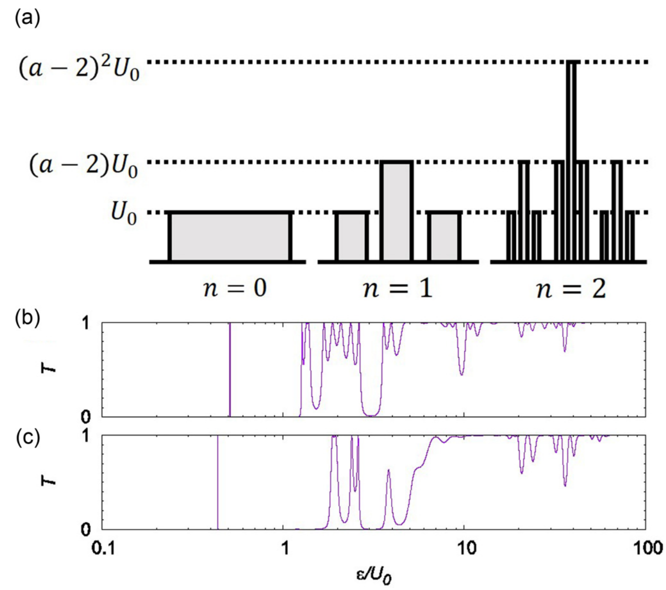

FIG. 8. Cantor-like potential where the potential height is not constant and the numerical calculation result is at $L=1$, $U=512$, $n=10$, $a=4$. (a) Schematic diagram of the Cantor-like potential in the $n=$ zeroth, first, and second, where the potential height is not constant. (b) Numerical result when the potential height is constant. (c) Numerical result when the potential height is not constant.

N^2 at $x = m'\pi$ (m' is an integer), and the submaximal value at x that satisfies $\tan(Nx)/[N\tan(x)] = 1$.

Second, the period of the extreme values of $G(k)$ is $\Delta k = (a/2\gamma)\pi$. This is because

$$\frac{\sin^2(m\pi)}{\sin^2(m\pi/N)}\frac{\sin^2(m\pi/a)}{\sin^2(m\pi/Na)}\cdots = 0,$$

and therefore $G(k)=0$ at $k = (\pi a/\gamma N)l$ (l is an integer other than a multiple of N), and $G(k)$ takes the extreme value at $k = \pi a/(\gamma)l'$ (l' is an integer). Figure 9 plots the behavior of $G(k)$ for various values of a and N. $G(k)$ takes the extreme values periodically in a logarithmic scale. The peaks appear at $k = \pi a^l y$, where l is an integer and y is a constant determined by a, N. Table I summarizes the values of peaks and y for various a and N.

The position of the first peak to the third peak follows the following rule. The first peak appears at $k = \pi \times a^l \times (N-1)/(a-1)$. The second peak appears at $k = \pi \times a^l \times (N-1)/a$ and the third peak appears at $k = \pi \times a^l \times (a+1)/a^2$. These rules are satisfied for any a's at $N=2$, however, there are other peaks that do not satisfy these rules at $N \neq 2$.

Third, the function $G(k)$ has multifractal properties. To examine the multifractality of $G(k)$, we calculated $G(k)^q$ in the interval $[a^{l-1}, a^l]$ [18,22,23],

$$F_q(l) = \int_{a^{l-1}}^{a^l} G(k)^q dk. \tag{31}$$

Table II summarizes the values of r_q for various values of a and N. The function $F_q(l)$ increases r_q^l exponentially with respect to l, and $r_1 = a/N$ for any a,N. At $N=2$, $r_2 = (3/8)\times a$ for any a. Additionally, for $q=0$, $r_0 = a$, and for sufficiently large q, $r_q \sim 1$.

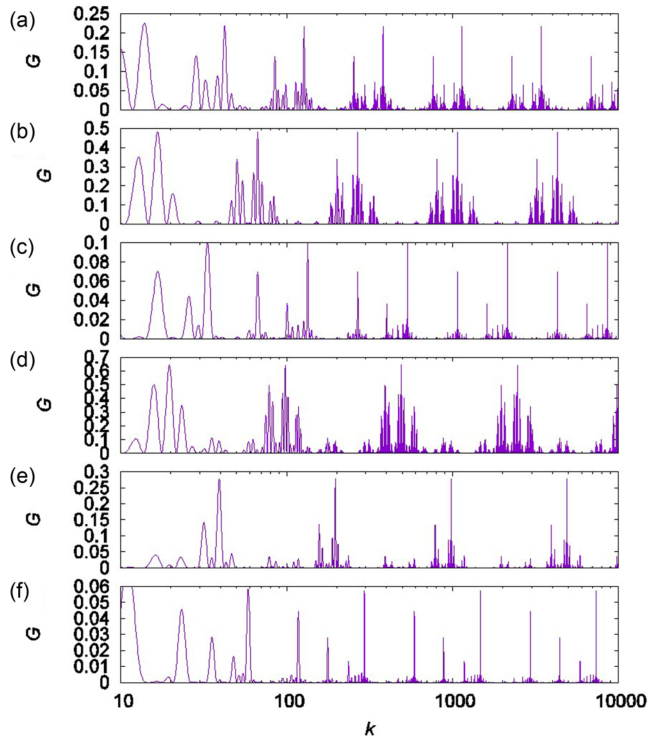

FIG. 9. $G(k)$ in a semilogarithmic scale of k. (a) $a = 3$, $N = 2$. (b) $a = 4$, $N = 2$. (c) $a = 4$, $N = 3$. (d) $a = 5$, $N = 2$. (e) $a = 5$, $N = 3$. (f) $a = 5$, $N = 4$.

In order to characterize the multifractality, the probability density in the interval $[a^{l-1},a^l]$ is defined as $p(k) = G(k)/\int_{a^{l-1}}^{a^l} G(k)dk = G(k)/F_1(l)$. A partition function Z_q is defined as

$$Z_q(l) = \int_{a^{l-1}}^{a^l} p^q(k)dk = \frac{\int_{a^{l-1}}^{a^l} G(k)^q dk}{[F_1(l)]^q} = \frac{F_q(l)}{[F_1(l)]^q}. \quad (32)$$

The generalized dimension D_q is defined as

$$D_q = \frac{1}{q-1}\frac{\ln[Z_q(l+1)] - \ln[Z_q(l)]}{\ln(1/a)}. \quad (33)$$

For sufficiently large m, the distribution function increases according to r_q^l/r_1^{lq}, so the generalized dimension can be written as

$$D_q = \frac{1}{q-1}\frac{q\ln r_1 - \ln r_q}{\ln a}. \quad (34)$$

TABLE I. The value of $G(k)$ from the first peak to the fourth peak for various a and N. The values in parentheses indicate $y = k/\pi a^l$.

a,N	1st peak	2nd peak	3rd peak	4th peak
3,2	$0.2174(\frac{1}{2})$	$0.1380(\frac{1}{3})$	$0.0705(\frac{4}{9})$	$0.0635(\frac{7}{18})$
4,2	$0.4780(\frac{1}{3})$	$0.3376(\frac{1}{4})$	$0.2546(\frac{5}{16})$	$0.2361(\frac{21}{64})$
4,3	$0.0993(\frac{2}{3})$	$0.0701(\frac{1}{3})$	$0.0362(\frac{8}{16})$	$0.0144(\frac{40}{64})$
5,2	$0.6417(\frac{1}{4})$	$0.4973(\frac{1}{5})$	$0.4303(\frac{6}{25})$	$0.4176(\frac{31}{125})$
5,3	$0.2779(\frac{2}{4})$	$0.1384(\frac{2}{5})$	$0.0873(\frac{12}{25})$	$0.0794(\frac{62}{125})$
5,4	$0.0574(\frac{3}{4})$	$0.0445(\frac{3}{10})$	$0.0279(\frac{9}{20})$	$0.0131(\frac{75}{125})$

TABLE II. r_q and generalized dimension for various a,N.

a,N	r_0	r_1	r_2	D_0	D_1	D_2
3,2	3.00000	1.50001	1.12503	1.00000	0.75722	0.63075
4,2	4.00000	2.00000	1.50000	1.00000	0.76618	0.70751
4,3	4.00001	1.33333	1.03182	1.00000	0.59925	0.39251
5,2	5.00000	2.49983	1.87497	1.00000	0.81448	0.74804
5,3	5.00000	1.67155	1.17906	1.00000	0.67147	0.53614
5,4	5.00000	1.24992	1.01242	1.00000	0.49076	0.26962

For $q = 0$, $D_0 = (-1)[-\ln(a)]/\ln(a) = 1$, since $r_0 = a$. At $N = 2$, $D_2 = [2\ln(a/2) - \ln(3a/8)]/\ln(a) = \ln(2a/3)/\ln(a)$ for any a. For sufficiently large q, $D_q = q/(q-1)[1 - \ln(N)/\ln(a)]$. Table II shows r_q and D_q ($q = 0$, 1, and 2) for various values of a and N. The generalized dimension D_q takes different values depending on a and N. This means that the function $G(k)$ has a different multifractality depending on a,N. In order to verify this, we calculated the $f(\alpha)$ spectrum by using the relation

$$\alpha(q) = \frac{d}{dq}[(q-1)D_q], \quad f(\alpha) = q\alpha(q) - (q-1)D_q. \quad (35)$$

For large q, α approaches $\alpha = [1 - \ln(N)/\ln(a)]$, because $D_q = q/(q-1)[1 - \ln(N)/\ln(a)]$ for large q. Figure 10 shows the $f(\alpha)$ spectrum for various a and N. Figure 10(a) compares $f(\alpha)$ spectra for $a = 3,4,5$ at $N = 2$. For $a = 4$, the spectrum is narrower than the case of $a = 3$ and 5. The width of the $f(\alpha)$ spectrum is narrow at $N = 2$ when a takes an even number. On the other hand, Fig. 10(b) compares the $f(\alpha)$ spectra for $N = 2,3,4$ at $a = 5$. There is no noticeable difference, although the width of $f(\alpha)$ becomes slightly larger with N. This trend is similarly observed at any a.

V. SUMMARY

We found that the transmittance for the generalized Cantor-like potential can be expressed using Chebyshev polynomials of the second kind, and for sufficiently large k, it is characterized by the finite product of the Laue function $G(k)$, which is a natural generalization of the finite product

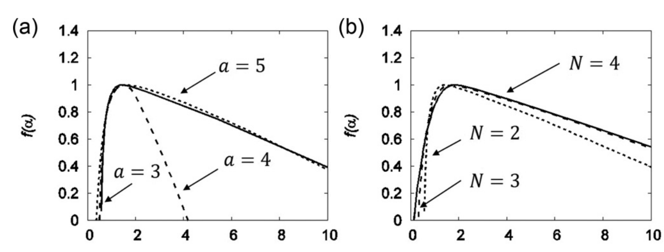

FIG. 10. (a) $f(\alpha)$ spectra at $a = 3$, 4, and 5 for a fixed value of $N = 2$. The solid line is $a = 3$, the dashed line is $a = 4$, and the dotted line is $a = 5$. (b) $f(\alpha)$ spectra at $N = 2$, 4, and 5 for a fixed value of $a = 5$. The solid line is $N = 4$, the dashed line is $N = 3$, and the dotted line is $N = 2$.

of the cosine function for the 3-adic Cantor-like potential. $G(k)$ is derived from the width of the gap in the Cantor-like potential of generation n, and takes peak values periodically in a logarithmic scale of k. Furthermore, $G(k)$ shows various multifractal properties depending on two parameters a and N.

A function expressed with the finite product such as $G(k)$ might appear even in other types of nontrivial potentials such as Fibonacci potentials. In the future, we would like to check whether the transmittance can be characterized by functions such as $G(k)$ even in these potentials.

[1] S. Alexander and R. Orbach, J. Phys. (Paris) **43**, 625 (1982).

[2] T. Nakayama, K. Yakubo, and R. L. Orbach, Rev. Mod. Phys. **66**, 381 (1994).

[3] E. Domany, S. Alexander, D. Bensimon, and L. P. Kadanoff, Phys. Rev. B **28**, 3110 (1983).

[4] X. R. Wang, Phys. Rev. B **51**, 9310 (1995).

[5] M. W. Takeda, S. Kirihara, Y. Miyamoto, K. Sakoda, and K. Honda, Phys. Rev. Lett. **92**, 093902 (2004).

[6] X. Sun and D. L. Jaggard, J. Appl. Phys. **70**, 2507 (1991).

[7] V. V. Konotop, Z. Fei, and L. Vázquez, Phys. Rev. E **48**, 4044 (1993).

[8] M. D. Noskov and A. V. Shapovalov, Russ. Phys. J. **36**, 703 (1993).

[9] C.-A. Gurein and M. Holschneider, J. Phys. A **29**, 7651 (1996).

[10] A. V. Lavrinenko, S. V. Zhukovsky, K. S. Sandomirski, and S. V. Gaponenko, Phys. Rev. E **65**, 036621 (2002).

[11] N. Hatano, J. Phys. Soc. Jpn. **74**, 3093 (2005).

[12] K. Honda and Y. Otobe, J. Phys. A **39**, L315 (2006).

[13] J. A. Monsoriu, F. R. Villatoro, M. J. Marin, J. Pérez, and L. Monreal, Am. J. Phys. **74**, 831 (2006).

[14] N. L. Chuprikov, J. Phys. A **33**, 4293 (2008).

[15] F. R. Villatoro and J. A. Monsoriu, Phys. Lett. A **372**, 3801 (2008).

[16] K. Esaki, M. Sato, and M. Kohmoto, Phys. Rev. E **79**, 056226 (2009).

[17] R. Sato, K. Kaino, and J. Sonoda, IEICE Trans. Electron. **E99-C**, 801 (2016).

[18] H. Sakaguchi and T. Ogawana, Phys. Rev. E **95**, 032214 (2017).

[19] See, e.g., D. W. L. Sprung, H. Wu, and J. Martorell, Am. J. Phys. **61**, 1118 (1993).

[20] H. Yamamoto, Y. Kanie, A. Kurita, and K. Taniguchi, Jpn. J. Appl. Phys. **34**, 4529 (1995).

[21] See, e.g., X. R. Wang, Phys. Rev. B **53**, 12035 (1996).

[22] H. G. E. Hentschel and I. Procaccia, Physica D **8**, 435 (1983).

[23] T. C. Halsey, M. H. Jensen, L. P. Kadanoff, I. Procaccia, and B. I. Shraiman, Phys. Rev. A **33**, 1141 (1986).